Available online at www.sciencedirect.com
ScienceDirect
Journal of Hazardous Materials 147 (2007) 618–624
Journal of Hazardous Materials
www.elsevier.com/locate/jhazmat

Filtration of nano-particles by a gas–solid fluidized bed

Kuang-Yu Liu [b], Ming-Yen Wey [a,*]

[a] Department of Environmental Engineering, National Chung-Hsing University, Taichung 402, Taiwan, ROC
[b] Department of Safety, Health and Environmental Engineering, National United University, Miao-Li 360, Taiwan, ROC

Received 8 September 2006; received in revised form 15 January 2007; accepted 15 January 2007
Available online 20 January 2007

Abstract

The filtration of 80 nm SiO_2 and Al_2O_3 particles in a gas stream using fluidized beds was studied. Silica sand and activated carbon (A.C.) were adopted as bed materials to filtrate 80 nm SiO_2 and Al_2O_3 particles. The collected particles were elutriated from the fluidized bed, so the filtration was a dynamic process and the variations of the removal efficiency with time were studied.

Experimental results showed that the filtrations of 80 nm SiO_2 and Al_2O_3 particles with a bed material of silica sand were not dynamic processes but the filtration by A.C. was. The removal efficiencies for SiO_2 and Al_2O_3 particles using silica sand as bed material were held steady and found to be equal, between 86 and 93%. A.C. is considered to be more efficient than silica sand because it has a high specific surface area. However, the experimental data yield conflicting results. The removal efficiency of Al_2O_3 particles fell from 92% initially to 80% at the end of test—a little lower than that obtained by filtration using silica sand. A higher voidage of A.C. than silica sand weakens the removal of nanoparticles since the diffusion mechanism dominates. The removal efficiency of SiO_2 by A.C. decayed from 83 to 40% with time passed. The huge differences between the filtration efficiency of SiO_2 and that of Al_2O_3 particles by A.C. was associated with the extensive segregation of SiO_2 and A.C. particles, which caused more SiO_2 particles to move to the top of the bed, where they were elutriated. The weak inter-particle force for SiO_2 decreased the removal efficiency also.

Keywords: Fluidized bed; Nanometer particles; Particle filtration; Segregation

1. Introduction

The production and use of nanometer materials in industrial manufacturing and research have attracted marked interest over recent years. However, the air pollution problem and an industrial safety hazard sometimes arise from the nanoparticles that are produced in industrial processes. For instance, the tail gas from a chemical vapor deposition process in the semiconductor industries has ultra-fine particles like silane and silicon dioxide [1]. Silane is a hazardous material and the deposition of such particles on the duct of the exhaust gas increases the danger of back-firing and explosion. Gas pollutants, such as inorganic acids and bases and organic vapors, must be removed at the same time as particles [2]. The removal of nanoparticles from the exhaust gas is a new area of research. Among traditional air pollution control devices, the bag filter, the electrostatic precipitator and the venturi scrubber are three highly efficient devices which are particularly used to remove the submicron particles in the industry. The main problems of the venturi scrubber are its high energy consumption and low efficiency of removal of nanoparticles. The electrostatic precipitator is associated with a risk of fire and explosion when flammable particles are handled [3]. When a bag filter is used to filter ultra-fine particles, the pressure drop is very large so the bags must be cleaned frequently [4]. Therefore, equipment to control the capture of nanoparticles must be developed.

The fluidized bed has the advantages of a uniform bed temperature, a high contact surface area and high mass/heat transfer efficiency so it is a popular device for a reaction between gas/solid phases. Some researchers have focused on the efficiency of particle filtration by fluidized beds with reference to various parameters, such as superficial gas velocity, static bed height, various collector particles, distributor types and the operating temperature [5–7]. Most have used a particle generator to produce monodispersed particles, typically with a diameter of around 1 μm. Some mathematical models have been proposed

* Corresponding author. Tel.: +886 4 22852455; fax: +886 4 22862587.
E-mail address: mywey@dragon.nchu.edu.tw (M.-Y. Wey).

0304-3894/$ – see front matter © 2007 Elsevier B.V. All rights reserved.
doi:10.1016/j.jhazmat.2007.01.058

to calculate the collection efficiency [8–10]. These models and experiments are developed specifically to eliminate the influence of the elutriation of particles. The removal of nanoparticles was beyond the scope of these studies. Tardos et al. [11] used a numerical solution to the diffusion equation to calculate a single sphere efficiency of sub-micron particles in fluidized beds. The results show that the removal efficiency increased as the particle size dropped in the sub-micron range, because of the Brownian effect. However, such small particles are not nanoparticles.

The filtration of nanoparticles by fluidized beds is not very well understood and very few studies have addressed it. The nanoparticles are very small and the diffusion mechanism dominates, so the fluidized bed can capture nanoparticles. In the authors' earlier works, the fluidized bed was used to remove acid gas, organic compounds and heavy metals [12–14]. A series studies also focused on the filtration of the fly ash of a coal-fired power plant and a municipal solid waste incinerator by fluidized beds [15–17]. This paper, one of these serious studies, examined the feasibility of the filtration of 80 nm particles by fluidized beds. In this work, the evaluated parameters are: (1) the species of the bed materials (silica sand and activated carbon) and (2) the species of the filtered particles (80 nm SiO_2 and Al_2O_3). The high surface area of A.C. may contribute to the high efficiency via diffusion. SiO_2 particles in the exhaust gas of the semiconductor industry cause operating problems. Of course, the removal of particles by a fluidized bed is complex. The collecting mechanisms of particles by the bed material, such as impaction, interception and diffusion, etc., are related to the capture of particles. The rebound and attrition of particles, the hydrodynamics, including flow regime, bubble size, bubble velocity, segregation and other factors, all affect the efficiency of removal. The aim of this study is to propose a new application of the fluidized bed to filter nanoparticles. The work involves no intense discussion of capturing mechanisms or mathematics.

2. Experimental

2.1. Apparatus and the materials

The experimental system was modified from the authors' previous work [17] and was schematically depicted in Fig. 1. A blower in front of the facility and a fan at the end supplied air; the flow rate was controlled using a valve and measured by a calibrated rotameter. The particles were pushed into the inlet gas by a powder feeder that was comprised of an outer tube, a driving motor and a screw threaded rod with a scale. A rapping system was mounted on the distributor and the inlet duct to avoid the adhesion of particles to the wall or distributor. A particle sampling train was installed at the outlet of fluidized bed reactor. A bypass was installed in front of the induced fan to maintain a constant pressure of the fluidized bed because different bed materials were employed.

Silica sand and A.C. were applied as bed materials. The silica sand with a size of 701–840 μm and a density of 2650 kg/m^3 was used in the test. Commercial A.C. (G840, China Activated

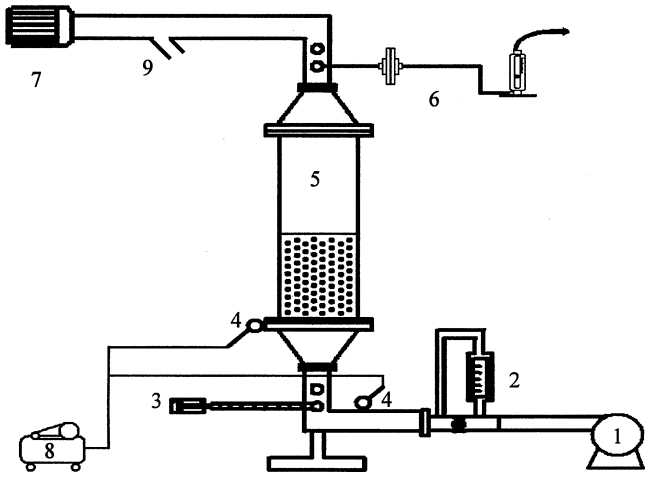

Fig. 1. Fluidized bed reactor: (1) blower; (2) flow meter; (3) powder feeder; (4) rapping system; (5) fluidized bed; (6) sampling train; (7) induced fan; (8) air compressor; (9) bypass.

Carbon Industries Ltd., Taipei, Taiwan) with a particle size of 1190–1410 μm and a density of 1360 kg/m^3 was another bed material. A.C. is a porous material with a large specific surface area, and may be useful in capturing the nanoparticles because it has more adhesion sites than silica sand for the particles. SiO_2 and Al_2O_3 particles with a diameter of 80 nm were used as filtered particles. Results for Al_2O_3 were compared with those of SiO_2 particles of the same size, because their other characteristics differ. Commercial SiO_2 and Al_2O_3 particles (Desunnano Co. Ltd., Taipei, Taiwan) were purchased for use in the test.

2.2. Experimental procedure

2.2.1. Performance of the filter in collecting 80 nm particles

In this study, a Whatman GF/A glass microfibre filter was used to extract the samples after they passed through the fluidized bed, to determine the exit concentration of the nanoparticles. However, the Whatman Company does not specify the performance of such filters in collecting nanoparticles. Therefore, the performance of the filter in collecting 80 nm particles was pre-tested. In the pre-test, the bed materials were not put into the fluidized bed and the distributor was dismounted. The apparatus was warmed up for 10 min and then 80 nm SiO_2 and Al_2O_3 particles were individually injected into the empty fluidized bed using a powder feeder. In the exit, two filters were used in series to collect SiO_2 or Al_2O_3 particles. The mass collected in the individual filter divided by the total mass collected in both filters is defined as the collection efficiency of the filter. Table 1 presents the collecting performance of the filter. The experimental results showed that the collection efficiencies of the first filter all exceeded 99% for both SiO_2 and Al_2O_3 in two runs. The extremely high efficiency indicated that the filter can effectively collect nanoparticles so one filter sufficed.

2.2.2. Filtration of 80 nm SiO_2 and Al_2O_3 with silica sand as bed material

Elutriation from fluidized beds is the carryover of the fine particles into the exit gas stream. The bed materials can always

Table 1
Performance of the fiberglass filter for 80 nm nanoparticles

	First run		Second run	
	First filter	Second filter	First filter	Second filter
SiO_2 mass (g) collection efficiency (%)	0.01751 (99.0)	0.00018	0.01808 (99.6)	0.00008
Al_2O_3 mass (g) collection efficiency (%)	0.04757 (99.9)	0.00007	0.04689 (99.9)	0.00050

be elutriated from the fluidized bed to be collected by the filter. The elutriated bed material represents the background mass and must be subtracted from the total mass of the collected particles in the filtration test. Hence, the elutriation test is undertaken before the nanoparticles are filtered.

Before the elutriation test was conducted, the inner column of the fluidized bed and all apparatus were cleaned to prevent errors during the experiment. The silica sand was placed into the reactor to a static height of 21 cm. The air-flow rate was fixed at 550 L/min at the temperature in the room, corresponding to a superficial velocity of 0.49 m/s. The fluidized bed was kept running for 6 h without adding the filtered particles. The test was sampled hourly for 6 h, until steady elutriation was reached. Then, the filtration of the nanoparticles was tested without replacing the silica sand after the elutriation test.

After the elutriation test, the weighed SiO_2 or Al_2O_3 particles were put into the powder feeder in individual tests, before being injected into the fluidized bed. The rapping system began to knock the distributor plate and the inlet duct, to prevent the particles from sticking to their surfaces, just before the particles were input. The rapping system worked also at the sampling time of elutriation tests, keeping the consistency of sampling procedures at the elutriation and filtration tests. After the experiment, the distributor plate and inlet duct were dismounted and the particles on them were weighed and their mass subtracted from the input mass. The driving speed of the particle feeder was regulated to a constant input rate of 66.2 ± 2.0 mg/min for SiO_2 and 126.8 ± 9.0 mg/min for Al_2O_3. The fact that the input rate of Al_2O_3 exceeded that of SiO_2 was attributed to its higher density and lower packing voidage. Reducing the feeder's speed to reduce the input rate of Al_2O_3 was attempted as it was for SiO_2, but the constant input cannot be achieved because the driving speed was too low. The input particle concentration was determined by dividing the input rate by the air flow rate of 550 L/min. Isokinetic sampling at the outlet of the fluidized bed filter was undertaken. The period of each sampling was 10 min and renewal of the filter took 3 min. These tasks were repeated for a total run time of 50 min and four samples were gathered in the test. The filters that contained nanoparticles were weighed and the masses compared with the masses of the filters before experiment. Each experiment was tested three times to check the consistency of data.

2.2.3. Filtrations of 80 nm SiO_2 and Al_2O_3 with A.C. as bed material

When A.C. was used as the bed material, the static height and air flow rate were the same as in the silica sand test. The duration of the elutriation test was also initially set to 6 h. However, pieces of granular A.C. were elutriated after the long-delayed attrition. A.C. has low hardness and is irregularly shaped so its attrition and elutriation were stronger than those of silica sand. The collection of a piece of granular A.C. by the filter causes significant errors in the outlet concentration. Accordingly, the elutriation test procedure was modified. The bed material was fluidized for an hour to warm up. The samples were then extracted at intervals of 10 min for a total of 2 h; the sampling time was 5 min: samples were obtained from 2 to 7 min in each interval. The run time of the filtration test was set to 50 min; a longer duration of 2 h was used for the designed elutriation test. Following the elutriation test, the A.C. was replaced with the new A.C. and then the filtration test was begun. After an hour of warming up, the SiO_2 or Al_2O_3 particles were injected into the bed, and samples were taken every 10 min for a total period of 50 min. The mass of the collected nanoparticles was determined by subtracting the mass of the elutriated A.C. from the total mass collected in the filter. The operating parameters and procedures in the filtration test were the same as in the silica sand test. The elutriation and filtration tests were all conducted three times. Table 2 lists the experimental conditions and characteristics of the materials used herein.

3. Results and discussion

3.1. Elutriation of the bed materials

In this work, silica sand and A.C. were used as the bed materials. Fig. 2 separately plots the elutriated concentration of the silica sand and A.C. with time. The error bar plot represents the mean concentration and the standard deviation from the three runs. The elutriation of silica sand was heavy at the beginning of the 4 h period and then steadily dropped as the time increased, as presented in Fig. 2(a). The concentration declined from around 37 mg/m^3 originally to a steady value of 20 mg/m^3,

Table 2
Experimental conditions and materials

Fluidized bed: 15.5 cm in diameter, 80 cm in height	
Static height: 21 cm	Temperature: 40–44 °C
Gas flow rate: 550 L/min	Gas velocity: 0.49 m/s
Bed materials: silica sand	Bed materials: activated carbon
Particle size: 701–840 μm	Particle size: 1190–1410 μm
Density: 2650 kg/m^3	Density: 1360 kg/m^3
Voidage (ε): 0.43	Voidage (ε): 0.63
U/U_{mf}: 1.38	U/U_{mf}: 1.22
Input particle: 80 nm SiO_2	Input particle: 80 nm Al_2O_3
Density: 2450 kg/m^3	Density: 3900 kg/m^3
Feed rate: 66.2 ± 2.0 mg/min	Feed rate: 126.8 ± 9.0 mg/min
Input concentration: 120.3 ± 3.6 mg/m^3	Input concentration: 230.6 ± 16.4 mg/m^3

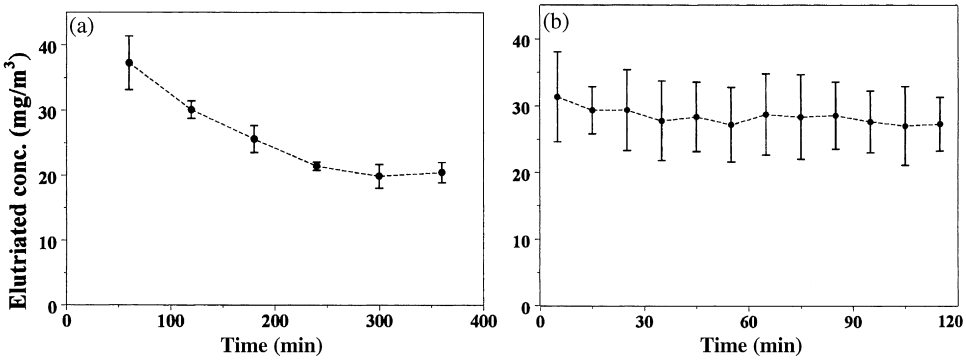

Fig. 2. The elutriated concentration of the various bed materials: (a) silica sand with clutriation time of 6 h and (b) A.C. with time of 2 h.

after 4 h. Hence, this value was set as the background concentration in the filtration test of nanoparticles. For the elutriation test of A.C., the elutriated concentration varied little during the operating time of 2 h, as shown in Fig. 2(b). The mean concentration fell from 31 mg/m^3 initially to a steady value of 27 mg/m^3 after 30 min. These various concentrations in each 10 min cycle during the first 50 min determined the background concentration of the elutriated A.C. in the filtration experiment and were subtracted from the exit concentration. The elutriated mass concentration of silica sand and A.C. did not differ much. However, the density of silica sand is about double that of A.C. so the elutriated counts of A.C. were higher than those of silica sand. The elutriated counts of A.C. overcomes silica sand, so the sampling time of A.C. is shorter (5 min) than that of silica sand (10 min), to prevent errors associated with the deposition of many particles in the filter and some particles may be rebounded.

Notably, the higher elutriation of A.C. fines than of silica sand, and the exit of some granular A.C. from the bed after a long time, causes problems if the fluidized bed is employed in real applications in industry. The elutriated concentration of bed material is considered as the background value in studies. However, the exit concentration increases with elutriation in real applications and violation of the emission standards must be considered. Of course, a cyclone or other control equipment can be employed to collect the particles elutriated from the bed. The elutriated particles increase the solid loading of downstream facilities.

3.2. Variations in outlet concentration of SiO_2 and Al_2O_3 with time

As aforementioned, a filter can effectively capture nanoparticles in the exhaust gas so only a filter is used in the sample

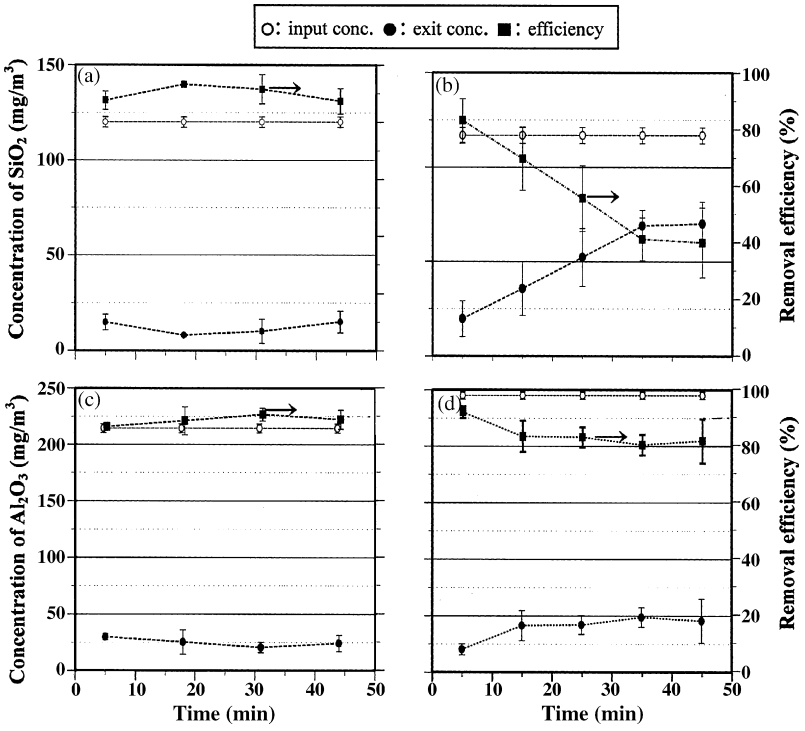

Fig. 3. The input, exit concentrations and removal efficiency of SiO_2 and AljOj with various bed materials: (a) SiO vs. silica sand; (b) SiO_2 vs. A.C.; (c) Al_2O_3 vs. silica sand; (d) Al_2O_3 vs. A.C.

train. The error bar plots in Fig. 3(a and b) refer to the filtration of 80 nm SiO_2 using the various bed materials. The background concentrations of the elutriated bed materials were subtracted from the outlet concentration. The mean input concentration of SiO_2 in three reruns was 123 mg/m^3 when silica sand was used as the bed material, as presented in Fig. 3(a). The outlet concentrations of SiO_2 ranged from 8 to 15 mg/m^3, varying a little with operating time. Fig. 3(b) depicts the test using A.C. as the bed material. The mean input concentration was 117 mg/m^3, a little lower than that in the test of silica sand, but the outlet concentrations obtained using A.C. were higher. Although the fluctuation of the outlet concentration during the three runs of the A.C. test was high, the mean value increased from 20 mg/m^3 initially to a steady concentration of 70 mg/m^3 finally. Fig. 3(c and d) shows the filtration of Al_2O_3. The input concentrations in the tests of silica sand and A.C. were 217 and 245 mg/m^3, respectively. The input concentrations of Al_2O_3 are higher because its density is higher than SiO_2. The mean outlet concentrations of the test of silica sand were 21–30 mg/m^3 and were independent of the operating time. In the tests of activated carbon, the concentrations increased from 20 to around 50 mg/m^3 with time.

3.3. Removal efficiency of SiO_2 and Al_2O_3

The changes of removal efficiency of SiO_2 and Al_2O_3 against time were also shown in Fig. 3. Because the elutriated concentration of the bed material was subtracted from the measured outlet concentration, the removal efficiency was the removal efficiency of the 80 nm SiO_2 and Al_2O_3 particles itself, not the efficiency of the fluidized bed device. Fig. 3(a and c) presents the removal efficiency of SiO_2 and Al_2O_3 with silica sand as the bed material. Within a total run time of 50 min, a steady efficiency of 86–93% was observed. Although the removal efficiency of SiO_2 slightly exceeded that of Al_2O_3, the difference is insignificant. If the removal efficiency of fluidized bed was discussed (i.e. the elutriated concentration of the bed material was included), the efficiency was 71–81%. However, the removal efficiencies of SiO_2 and Al_2O_3 when A.C. was used as the bed material differed considerably, as plotted in Fig. 3(b and d). The efficiency of the Al_2O_3 particles fell slightly from 92 to 80% with operating time, the removal efficiency of the fluidized bed decreased from 80 to 69%. However, the removal efficiency of SiO_2 was initially 83%, dropping sharply to 40% at the end and the removal efficiency of the fluidized bed decreased from 57 to 16%. The filtration of Al_2O_3 with A.C. is more effective than that of SiO_2, perhaps because Al_2O_3 is denser than SiO_2, so fewer of the Al_2O_3 particles that have been captured in the fluidized bed are elutriated once again. The other possibility is that the inter-particle forces between A.C. and Al_2O_3 are stronger than that between A.C. and SiO_2. The hamakar constant of SiO_2 and Al_2O_3 are 6.5 and 16.75 ($\times 10^{-20}$ J) individually. Therefore, the van der Waals force between Al_2O_3 and A.C. is higher than that for SiO_2. Comparing the efficiency of silica sand with A.C. as bed materials shows that the removal of Al_2O_3 using silica sand was slightly better than that using A.C. In the filtration of SiO_2, the difference between removal efficiencies increased with operating time. The removal of SiO_2 using A.C. is 10% lower than that using silica sand initially, but sharply declined to 40% finally. A.C. is associated with the initial lower removal efficiency than silica sand because A.C. has a high packed voidage. A high voidage weakens the removal of fine particles since the diffusion mechanism dominates [11].

The rapid drop in the efficiency of SiO_2 elucidates dynamic filtration [17]. The particles entered from the bottom and remained in the bed before binary mixture occurred. As time passed, more particles were captured and the segregation enhanced. The SiO_2 particles moved to the top of the bed and were elutriated to raise the exit concentration significantly. In an earlier work [16], the segregation of the binary mixture was proved to affect the filtration of particles of the incinerator fly ash. Al_2O_3 does not exhibit this phenomenon violently perhaps because its density is higher or the adhesive force between Al_2O_3 and Al_2O_3 particles or Al_2O_3 and A.C. particles is stronger than that with SiO_2 so the segregation is weaker.

3.4. Intensive analysis of the bed material of A.C.

As described above, filtering Al_2O_3 and SiO_2 using A.C. as the bed material differed greatly from doing so using silica sand. Moreover, A.C. is a porous material and the chemical element differs from silica sand (silica sand contains large amount of SiO_2 and Al_2O_3, but A.C. does not), so the clean A.C. (C.A.C.), A.C. filtered of SiO_2 (S.A.C.) and Al_2O_3 (A.A.C.) are intensively analyzed to clarify some facts.

3.4.1. BET test of A.C.

The A.C. is a porous material that has macro, meso and micropores. When the filtered SiO_2 and Al_2O_3 are attached to A.C., the pore structure is changed. In this test, 80 nm particles, which are much larger than the pores in A.C. are filtered. These large particles are expected to appear at the surface or to block the macropores of A.C., so the structures of macro, meso and micropores are all shifted. If smaller particles are filtered, then they block the smaller pores in A.C., so the macro and mesopores are less affected.

Table 3 presents the BET results of the C.A.C., S.A.C. and A.A.C. The total surface areas of C.A.C., S.A.C. and A.A.C. are 679.27, 457.86 and 525.85 m^2/g, respectively. The decline in the total surface areas of all types of A.C. explains the block in the pore structure, elucidating the capture of the 80 nm particles

Table 3
BET results of the various activated carbon

	Clean A.C.	A.C. with SiO_2	A.C. with Al_2O_3
Total surface area (m^2/g)	679.27	457.86	525.85
Surface area (micropore) (m^2/g)	607.25	412.50	478.93
Surface area (macro and mesopore) (m^2/g)	72.02	45.36	46.92
Micropore volume (cm^3/g)	0.2958	0.2022	0.2373
Macro and mesopore volume (cm^3/g)	0.3904	0.2704	0.3080

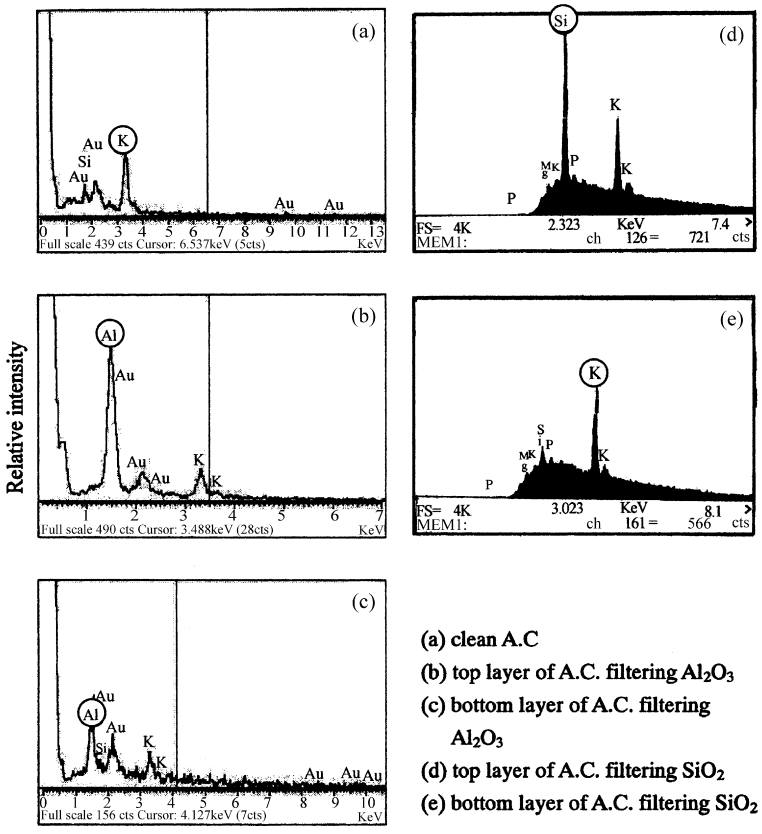

Fig. 4. EDS results of clean A.C., top and bottom layers of A.C. filtering particles.

by A.C.. The surface areas are 607.25, 412.50 and 478.93 m^2/g for micropores, and 72.02, 45.36 and 46.92 m^2/g for macro and mesopores. The drops in all of the pore size indicate that the filtered 80 nm SiO_2 and Al_2O_3 particles are attached to the large pores of the A.C. since they cannot enter the small pores. The surface areas of the macro and the mesopores of S.A.C. are equal but that of micropores is less than that of the pores in A.A.C., suggesting that the SiO_2 particles can be deposited on smaller pores than can Al_2O_3. Although the particle sizes of SiO_2 and Al_2O_3 are equal, the attrition, adhesion and other parameters of the different particles vary because their characteristics differ. SiO_2 particles may be attrited within the bed to small particles, or they do not coagulate with large particles, before entering the small pores.

3.4.2. X-ray energy dispersive spectrometer (EDS) test of A.C.

The SiO_2 and Al_2O_3 particles float to the top of the bed because their particles are much smaller than those of bed material, so the SiO_2 and Al_2O_3 contents in A.C. in the upper or bottom layer differ. After the filtration test had been completed, the A.C. of the top and bottom layers was individually collected, and the chemical composition of the A.C. was analyzed by X-ray EDS. The C.A.C. was also tested as the background. Fig. 4 shows the EDS results of C.A.C., and the top and bottom layers of A.A.C. and S.A.C. Fig. 4(a) depicted that the main constituents (excluding elements C and O) were K, Si and Au in the C.A.C., and K was most abundant. Au was employed as the coating film of EDS and so a corresponding peak was observed in the spectrum. The abundant element was K in C.A.C. but Al in A.A.C., as shown in Fig. 4(b and c), which fact explained the collection of Al_2O_3 particles. The intensity of Al in the top layer exceeded that in the bottom layer, confirming that more Al_2O_3 particles were present on the top. The EDS of S.A.C., as shown in Fig. 4(d and e), yielded the same results. Additionally, the intensity of Si in the top layer was extremely higher than that in the bottom layer, elucidating the extensive segregation for S.A.C. Segregation reduces the collection efficiency, especially for SiO_2 particles with weak inter-particle forces.

4. Conclusions

The removal of SiO_2 and Al_2O_3 particles with a size of 80 nm by fluidized beds is attainable. Variations in collection efficiency with time have different patterns, determined by the various bed materials and the filtered particles. If silica sand is applied as the bed material, then the efficiencies of both particles are approximately the same, 90%, and independent of the operating time. If the removal efficiency of the fluidized bed device was considered, the efficiency was 75% approximately when silica sand was applied as bed materials.

Filtering SiO_2 and Al_2O_3 particles using A.C. bed material is a dynamic process, whose efficiency decreases with operating time, but differences exist between SiO_2 and Al_2O_3 particles. The collection efficiency of Al_2O_3 fell slightly from 92 to 80%,

but declined greatly from 83 to 40% for SiO_2. The efficiency of the fluidized bed device fell from 80 to 69% for Al_2O_3 but decreased from 57 to 16% for SiO_2. The differences are attributed to the inter-particle force and extent of segregation in the fluidized bed. The strong inter-particle force enhances the adhesion of particles to form large particles or sticking to the bed material, so fewer particles are elutriated. The un-combined small particles form a binary mixture and move to the top, before segregation occurs. These small particles are easily blown out and leave the fluidized bed, reducing the removal efficiency. The elutriated bed materials reduce the removal efficiency of the fluidized bed because the outlet concentration rises. However, the elutriated bed materials are large in most cases and they are easily captured by other control devices.

References

[1] S.J. Lu, A numerical study of prediction venturi scrubbers performance, M.S. Thesis, National Chiao Tung University, Hsinchu, Taiwan, ROC, 2002.
[2] C.C. Huang, Emission characteristics of inorganic acid and base waste gas and control efficiency of packed towers in high-tech industry, M.S. Thesis, National Chiao Tung University, Hsinchu, Taiwan, ROC, 2002.
[3] Y.M. Wang, Experimental study of an efficient venturi scrubber, M.S. Thesis, National Chiao Tung University, Hsinchu, Taiwan, ROC, 2001.
[4] Y.H. Cheng, C.J. Tsai, Factors influencing pressure drop through a dust cake during filtration, Aerosol Sci. Technol. 12 (1998) 456–459.
[5] P. Knettig, J.M. Beeckmans, Capture of monodispersed aerosol particles in a fixed and in a fluidized beds, Can. J. Chem. Eng. 52 (1974) 703–706.
[6] Y. Doganoglu, V. Jog, K.V. Thambimuthu, R. Clift, Removal of fine particles from gases in fluidized beds, Trans. IChemE 56 (1978) 239–248.
[7] M. Ghadiri, J.P.K. Seville, R. Clift, Fluidized-bed filtration of gases at high temperatures, Trans. IChemE 71A (1993) 371–381.
[8] M.H. Peters, L.-S. Fan, T.L. Sweeny, Simulation of particulate removal in gas–solid fluidized beds, AIChE J. 28 (1982) 39–49.
[9] K. Ushiki, C. Tien, Calculation of aerosol collection in fluidized filter beds, AIChE J. 30 (1984) 156–168.
[10] K. Ushiki, C. Tien, Aerosol collection in the jet region of fluidized filters, AIChE J. 32 (1986) 1606–1611.
[11] G. Tardos, N. Abuaf, C. Gutfinger, Diffusion filtration of dust in a fluidized-bed, Atmos. Environ. 10 (1976) 389–394.
[12] B.C. Chiang, M.Y. Wey, W.Y. Yang, Control of incinerator organics by fluidized bed activated carbon adsorber, J. Environ. Eng. 126 (11) (2000) 985–992.
[13] B.C. Chiang, M.Y. Wey, C.L. Yeh, Control of acid gases using a fluidized bed adsorber, J. Hazard. Mater. 101B (2003) 259–272.
[14] B.C. Chiang, M.Y. Wey, W.Y. Yang, C.Y. Lu, Simultaneous control of metals and organics using fluidized bed adsorber, Environ. Technol. 24 (2003) 1103–1115.
[15] B.C. Chiang, M.Y. Wey, K.Y. Liu, Filtration of fly ash using a fluidized-bed filter, J. AWMA 55 (2005) 181–193.
[16] M.Y. Wey, K.H. Chen, K.Y. Liu, The effect of ash and filter media characteristics on particle filtration efficiency in fluidized bed, J. Hazard. Mater. 121B (2005) 175–181.
[17] K.Y. Liu, M.Y. Wey, Dynamic purification of coal ash by a gas–solid fluidized bed, Chemosphere 60 (2005) 1341–1348.